Scripta Materialia 223 (2023) 115056

Contents lists available at ScienceDirect

Scripta Materialia

journal homepage: www.journals.elsevier.com/scripta-materialia

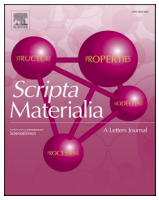

Decoupling between enthalpy and mechanical properties in rejuvenated metallic glass

S.Y. Zhang [a,b,1], W.H. Zhou [a,b,1], L.J. Song [c,d], J.T. Huo [c,d], J.H. Yao [a], J.Q. Wang [c,d], Y. Li [a,*]

[a] Shenyang National Laboratory for Materials Science, Institute of Metal Research, Chinese Academy of Sciences, Shenyang 110016, China
[b] School of Materials Science and Engineering, University of Science and Technology of China, Shenyang 110016, China
[c] CAS Key Laboratory of Magnetic Materials and Devices, and Zhejiang Province Key Laboratory of Magnetic Materials and Application Technology, Ningbo Institute of Materials Technology and Engineering, Chinese Academy of Sciences, Ningbo 315201, China
[d] Center of Materials Science and Optoelectronics Engineering, University of Chinese Academy of Sciences, Beijing 100049, China

ARTICLE INFO

Keywords:
Metallic glass
Rejuvenation
α-relaxation
β-relaxation
Differential scanning calorimetry

ABSTRACT

The mechanical properties of amorphous materials are closely related to their energy states (enthalpy). Usually, a higher energy state corresponds to larger plasticity and lower hardness. Here, we explore the correlation between the enthalpy and hardness of rejuvenated Au-based metallic glasses (MGs). We found that the rejuvenated MG with a high-energy state presents a hardness variation trend different from before, i.e. the hardness increases instead of keeping on decreasing with increasing enthalpy when the enthalpy is higher than an intermedia value. It is revealed that both the reactivations of β- and α-relaxation are beneficial to increasing the enthalpy but show opposite effect on the hardness. This study shows that this decoupling may be originated from the beginning of the reactivation of α-relaxation. Our work provides new insights into designing MGs with excellent mechanical properties by rejuvenating relaxed MGs via the furthest reactivation of β-relaxation and avoiding reactivation of α-relaxation.

Generally, the enthalpy of metallic glasses (MGs) is coupled with their mechanical properties, i.e., higher enthalpy corresponds to larger plasticity and lower hardness, and vice versa [1–11]. Therefore, the mechanical performance of MGs can be tailored by varying their enthalpy. In the relaxed state, usually obtained by sub-T_g (T_g, glass transition temperature) annealing, the MGs are in a low energy state and show high hardness and low plasticity [7,8]. On the other hand, in the rejuvenated state, for example after rejuvenation by cryogenic thermal cycling treatment, the energy states of MGs are lifted, and the rejuvenated MGs exhibit low hardness and improved plasticity/ductility [1,6,12–15].

Conventionally, structural relaxation of MGs is usually carried out by annealing at a temperature far below T_g where β-relaxation occurs [16]. The β-relaxation is thought to correspond to localized atomic rearrangements and results in a decrease in enthalpy and an increase in hardness [17]. On the other hand, it has been reported that reactivation of β-relaxation, recovery of the relaxed intrinsic flow units [18], can increase the enthalpy, improve the plasticity and simultaneously reduce the hardness of MGs. Hence, the observed coupling between enthalpy and mechanical properties is attributed to the β-relaxation and reactivation of β-relaxation which correspond to the local atomic rearrangement in soft regions [19,20] or flow units [16,21,22]. However, it is still unclear whether the reactivation of α-relaxation, which is corresponding to large-scale atomic rearrangement, can be achieved during rejuvenation at a temperature below T_g and its influence on the enthalpy and mechanical properties. As a consequence, another question that whether this coupling is still maintained when the reactivation of α-relaxation occurs is raised.

Here, we explore the effect of thermal rejuvenation on the enthalpy and hardness of the relaxed $Au_{50}Cu_{25.5}Ag_{7.5}Si_{17}$ MGs at a rejuvenation temperature ($T_{rej.}$) around but below T_g. An intriguing trend that the enthalpy increases monotonically with increasing rejuvenation temperature, while the hardness shows the minimum at the rejuvenation temperature of ~0.95 T_g was observed, implying a decoupling between enthalpy and hardness for samples rejuvenated at high rejuvenation temperatures. It is revealed that both the reactivations of β- and α-relaxation are beneficial to the increase in enthalpy, and that the reactivation of β-relaxation reduces the hardness as expected while the

* Corresponding author.
E-mail address: liyi@imr.ac.cn (Y. Li).
[1] These authors contributed equally to this work.

https://doi.org/10.1016/j.scriptamat.2022.115056
Received 18 July 2022; Received in revised form 12 September 2022; Accepted 15 September 2022
Available online 10 October 2022

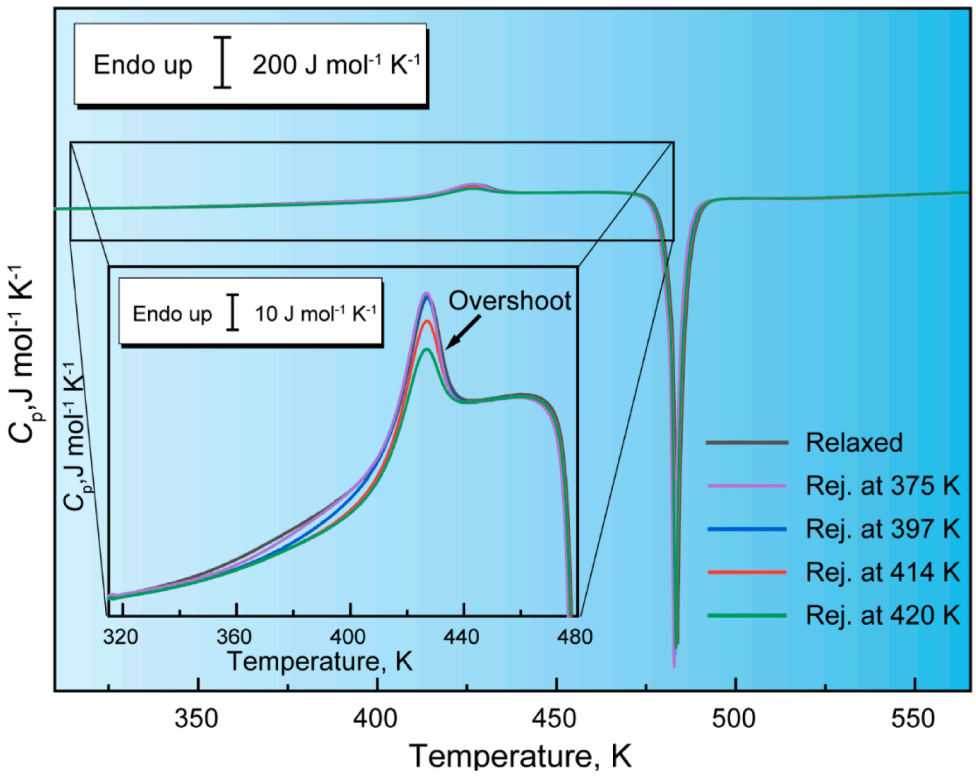

Fig. 1. Differential scanning calorimetry (DSC) traces of the relaxed sample and several representative rejuvenated samples at a heating rate of 100 K s^{-1}. The inset shows a close-up of around the glass transition.

reactivation of α-relaxation results in an increase in the hardness, showing that decoupling between enthalpy and mechanical properties is originated from the reactivation of α-relaxation. Our findings provide new insights into designing MGs with optimum mechanical properties by rejuvenating a relaxed MG via the furthest reactivation of β-relaxation and avoiding reactivation of α-relaxation.

The relaxation and rejuvenation of Au-based MGs were carried out by using a flash differential scanning calorimetry (Flash DSC 1, Mettler Toledo). A fully glassy sample was obtained by cooling a liquid at a cooling rate of $R_c = 1000$ K s^{-1}. The glass transition temperature T_g and crystallization temperature T_x are measured to be 420 K and 476 K, respectively, at a heating rate of 100 K s^{-1}. The relaxed MG was obtained by heating the MG to 438 K (within the supercooled liquid region) and then immediately cooling to 303 K at 3 K s^{-1}. Rejuvenation, increasing the enthalpy, was achieved in a second heating of the relaxed sample. The relaxed MG was heated to a different temperature ranging from 363 K to 420 K at 100 K s^{-1} and then immediately cooled at 1000 K s^{-1} to 303 K to obtain the rejuvenated MG. The measurement of heat flow was carried out at a heating rate of 100 K s^{-1}. The detail of the thermal protocol is shown in Fig. S1. The Vickers hardness testing (Q10 A+ microhardness tester) was conducted with a load of 15 g at room temperature. According to the ASTM MNL46 standard [23], the hardness value was calculated based on the length of the diagonals of the indentation that was analyzed by LEXT OLS4000 laser confocal microscopy. At least 4 samples were tested for each condition, and in order to minimize the influence of aging, the total time of sample fixing and polishing was limited to 3 min.

Fig. 1 shows the DSC traces of the relaxed sample and several representative rejuvenated samples. The inset shows the close-up of the DSC curves at the temperature range of 310 K-480 K. For the relaxed sample, its DSC curve exhibits an obvious endothermic peak, also known as *overshoot* peak that often observed in an annealed or slow cooled MG [24–26], at a temperature above T_g, demonstrating its low energy state. After rejuvenation, the value of specific heat C_p decreases at the

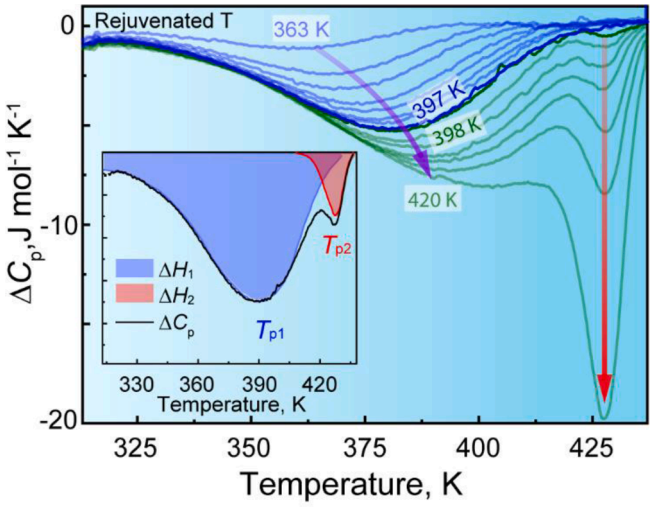

Fig. 2. Differences in the specific heat ΔC_p between the rejuvenated and relaxed samples. The purple and red arrows illustrate the variation of the two peaks respectively. The inset shows the ΔC_p curve of the sample rejuvenated at 408 K and its corresponding fitting curves with two distinct peaks (T_{p1} and T_{p2}). (For interpretation of the references to colour in this figure legend, the reader is referred to the web version of this article).

temperature range from ~320 K to 440 K compared with that of the relaxed sample, indicating a rejuvenation effect. With the increase in the rejuvenation temperature from 363 K to 420 K, the value of specific heat keeps on decreasing, implying a stronger rejuvenation effect at higher rejuvenation temperatures. However, it is noted that the specific heat curves show two obvious characteristic peaks for samples rejuvenated at different rejuvenation temperatures. For samples rejuvenated at a rejuvenation temperature lower than 397 K, only the value of specific

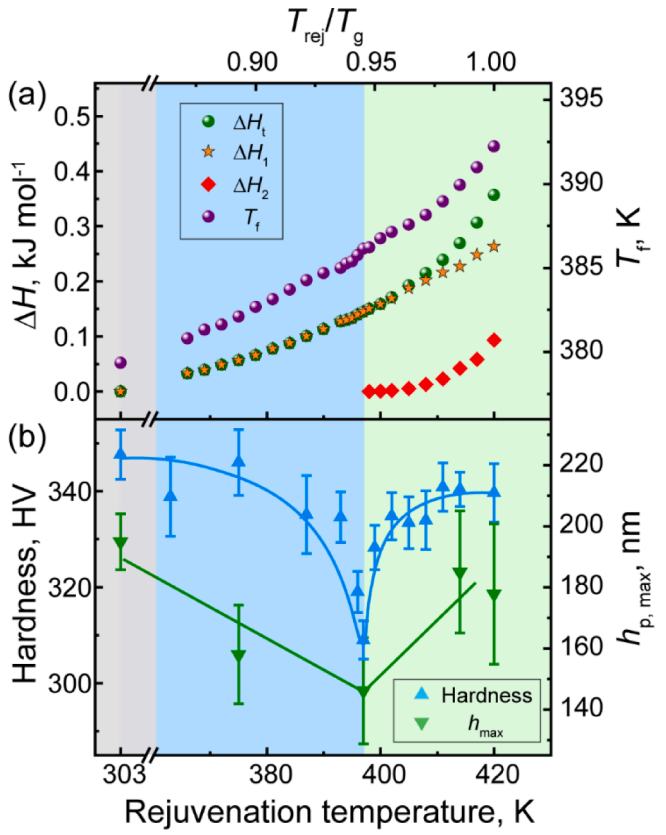

Fig. 3. (a) Enthalpy changes and fictive temperature as a function of rejuvenation temperature. (b) Hardness and maximum height of pile-up ($h_{p,\,max}$) as a function of the rejuvenation temperature. The error bars show the standard deviation for the hardness and $h_{p,\,max}$ measurements.

heat at low-temperature range (below T_g) decreases with increasing rejuvenation temperature, however, at higher temperature range (above T_g), the specific heat curves remain overlapped with that of the relaxed sample. For samples rejuvenated at a rejuvenation temperature higher than 397 K, the intensity of overshoot peak begins to decrease with increasing rejuvenation temperature.

To better illustrate the difference in the rejuvenated samples, all the C_p curves of rejuvenated samples were subtracted by that of the relaxed sample, and the corresponding differences in the specific heat, ΔC_p (= $C_{p,\,rejuvenated}$ - $C_{p,\,relaxed}$), are shown in Fig. 2. It is shown that the ΔC_p curves exhibit obvious difference for samples rejuvenated at different rejuvenation temperatures. For the samples rejuvenated at low rejuvenation temperatures (lower than 397 K), only one single peak exists on the ΔC_p curves, and the intensity of this peak increases with increasing rejuvenation temperature. However, when the rejuvenation temperature reaches 398 K, a second peak appears, and the intensity of the second peak also increases with increasing rejuvenation temperature. To clearly show the splitting, the ΔC_p curve of the sample rejuvenated at 408 K was fitted with two distinct peaks of T_{p1} and T_{p2} (inset in Fig. 2). The increasing intensity in the peaks demonstrates the increasing rejuvenation effect with the increasing rejuvenation temperature, however, the transition from one single peak to two separated peaks may imply different rejuvenation mechanisms at different rejuvenation temperatures.

To verify this, taking the sample rejuvenated at 408 K as an example, the activation energy, ΔE_1 and ΔE_2, of the two peaks was investigated at different heating rates varying from 40 K s^{-1} to 200 K s^{-1} as shown in Fig. S2. The ΔE_1 and ΔE_2 are determined to be (82.8 ± 1.5) kJ mol^{-1} and (168.6 ± 12) kJ mol^{-1}, respectively. Noted that the ΔE_1 is about (24 ± 0.5) RT_g, which is almost equal to the β-relaxation activation energy ΔE_β ≈ (26 ± 4) RT_g [27]. It has been demonstrated that the rejuvenation of relaxed MG at temperatures below T_g can be attributed to the reactivation of β-relaxation [18]. Hence, it is believed that the first peak in the ΔC_p curves is corresponding to the reactivation of β-relaxation during rejuvenating the relaxed sample at low rejuvenation temperatures. On the other hand, the ΔE_2 is about (48.3 ± 3.4) RT_g, which is close to the α-relaxation activation energy as reported by Song et al. [28]. Considering that the peak temperature T_{p2} of 428 K is higher than the T_g of 420 K, therefore, it is reasonable to speculate that the second peak in the ΔC_p curves in the samples rejuvenated at higher rejuvenation temperatures (inset in Fig. 2) is corresponding to the reactivation of α-relaxation during the rejuvenation process.

The difference in energy state between the rejuvenated samples and relaxed sample can be quantitative characterization by the enthalpy changes, ΔH, the integration of the corresponding ΔC_p curves. The total enthalpy changes, ΔH_t, as a function of rejuvenation temperature is shown in Fig. 3a. Considering that the ΔH_t consist of two parts: the reactivation of β-relaxation (ΔH_1, corresponding to the first peak in Fig. 2) and the reactivation of α-relaxation (ΔH_2, corresponding to the second peak in Fig. 2), ΔH_1 and ΔH_2 are calculated separately and the results are also plotted in Fig. 3a. It is shown that, when the rejuvenation temperature is lower than 397 K, only the reactivation of β-relaxation contributes to the increase in the energy state, hence, the ΔH_t and ΔH_1 are overlapped. With the further increase in the rejuvenation temperature, the reactivation of α-relaxation occurs, both the reactivation of β-relaxation and α-relaxation contribute to the rejuvenation and increase in energy state, resulting in the sharply increase in the ΔH_t.

The variation of energy state during rejuvenation may imply a variation of structure state which can be well characterized by the fictive temperature, T_f [29]. Here, the T_f is obtained from the intersection between the extrapolated glass and liquid lines (Fig. S3), and the corresponding results are also shown in Fig. 3a. Similar to the variation of energy state, the T_f increases monotonically with increasing rejuvenation temperature, showing a one-to-one correspondence in energy state and T_f as observed before [9,10,30–33], i.e. higher T_f corresponding to higher energy state, and *vice versa*.

It has been demonstrated that rejuvenation/high T_f is beneficial to mechanical properties, such as improving plasticity, fracture toughness and reducing hardness [1,9,10,30,34]. Here, the hardness of the relaxed and rejuvenated samples was also measured and the results are shown in Fig. 3b. The corresponding indentation morphologies are shown in Fig. S4. The relaxed sample shows the maximum hardness of 347 ± 5 Hv. After rejuvenation, the enthalpy and T_f increase (Fig. 3a), and as expected, softening occurs in all of the rejuvenated samples compared with that of the relaxed sample. However, contrary to the monotonic increase in enthalpy and T_f, the hardness does not evolve in a monotonic trend. It decreases firstly to a minimum value of 309 ± 4 Hv for the sample rejuvenated at 397 K, then increases gradually and reaches a maximum of 340 ± 5 Hv for the sample rejuvenated at 420 K. Although the plasticity was not investigated in present work due to the limited size of sample, the maximum height of pile-up ($h_{p,\,max}$), which can reflect the deformation mode and plasticity [2,35–38], was carefully measured. The minimum in $h_{p,\,max}$ of the sample rejuvenated at 397 K (Fig. 3b) may imply that it deforms more homogeneously and possesses the largest plasticity among all the relaxed and rejuvenated samples [37]. The monotonic increase in enthalpy and non-monotonic variation tendency of mechanical properties show a decoupling between enthalpy and mechanical properties. This decoupling can also be revealed by the non-monotonic correlation between hardness and fictive temperature as shown in Fig. S5.

It is believed that MG consists of soft regions (the weakly bonded regions) and hard regions (strongly bonded regions) [16,39]. The soft regions are also described as liquid-like regions, which have more free volume and are at a higher energy state, and thus it is well accepted that the higher energy state is, the more liquid-like regions exist and the lower hardness is in MG [2,9,40–42]. However, we observed an

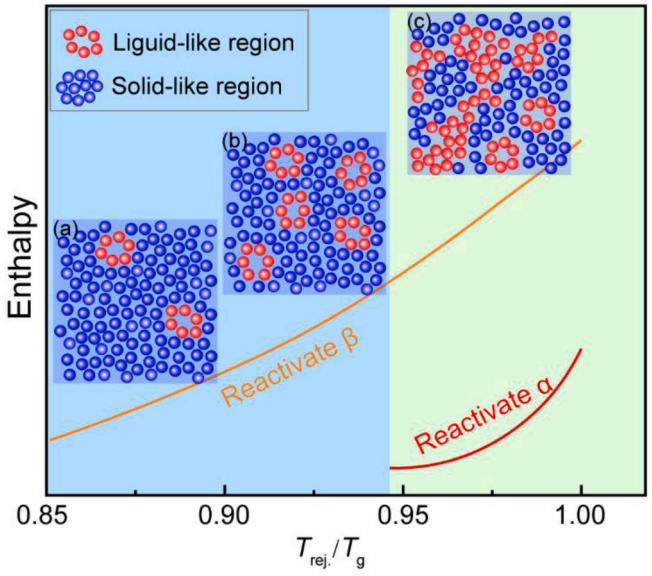

Fig. 4. Schematic of temperature-dependent enthalpy change and the evolution of microstructure.

abnormal phenomenon that a higher-energy state gives a harder glass. The decoupling between enthalpy and hardness during the rejuvenation of the relaxed samples can be understood from the distribution of liquid-like regions and special structural evolution as shown in Fig. 4.

In the present work, the relaxed MG is obtained at a low cooling rate of 3 K s^{-1}. During the slow cooling process, the free volume annihilates and thus the relaxed MG becomes harder and is at a low energy state. In the following rejuvenation at low temperatures, the specimen expands and generates liquid-like regions, and these high-energy defects are partially frozen in the subsequent quenching process at a cooling rate of 1000 K s^{-1}. This results in the reactivation of β-relaxation as suggested in Fig. 2 and Fig. 3a, and gives the increase in the fraction of liquid-like region annihilated during slow cooling, and therefore, results in the reduced hardness compared with that of the relaxed sample as observed in Fig. 3b. With the increasing of rejuvenation temperature to 397 K (~0.95 T_g), more sites of β-relaxation are reactivated and frozen in the MGs (inset (b) of Fig. 4), resulting in a continuous decrease in hardness.

Once the rejuvenation temperature is higher than 397 K but still below T_g, the isolated liquid-like regions connect with each other. This percolation of these liquid-like regions leads to large-scale structural rearrangement, inducing the reactivation of α-relaxation. Due to the rejuvenation temperature is still below T_g, the MG does not enter into the supercooled liquid region and hence these connected liquid-like regions are still wrapped by the solid-like matrix as shown in the inset (c) of Fig. 4. However, this large-scale structural rearrangement may provide an opportunity for the formation of chemical short-range order (CSRO), which is believed to have no influence on the energy state but have a significant influence on deteriorating the mechanical properties of MG [43,44]. Hence, the energy state continuously increases, but the hardness does not continuously decrease. Besides, the inhomogeneous expansion between the liquid-like regions and solid-like regions may induce significant internal stress, which can trigger a denser atomic packing (hard spots) in the solid-like regions as suggested by Zhu et al. [45], and in turn counteracts the softening effect to some extent. Both the formation of CSRO or hard spots weaken the ability of softening induced by the increasing liquid-like regions, and give the observed decoupling between the enthalpy and hardness. However, the exact nature of the atomic structure evolution during rejuvenation at different temperatures and its influence on the mechanical properties need further investigation.

In summary, we systematically investigated the rejuvenation behaviors of a slow-cooled Au-based MG including the changes in enthalpy and hardness. Contrary to the continuous increase in the energy state with the increasing rejuvenation temperature, the hardness of our rejuvenated samples exhibits a non-monotonic variation trend, showing decoupled behavior between the enthalpy and hardness at the rejuvenation temperature below T_g. The reactivation of β-relaxation softens the MGs, however, the reactivation of α-relaxation weakens the roles of β-relaxation. Our present results give a new insight into designing MGs with excellent mechanical properties by rejuvenating relaxed MGs via the furthest reactivation of β-relaxation and avoiding reactivations of α-relaxation.

Declaration of Competing Interest

The authors declare that they have no known competing financial interests or personal relationships that could have appeared to influence the work reported in this paper.

Acknowledgments

The authors acknowledge financial support from the Shenyang National Laboratory for Materials Science. Y. Li and J.Q. Wang acknowledge support from the National Natural Science Foundation of China (Grant no. 52231006).

Supplementary materials

Supplementary material associated with this article can be found, in the online version, at doi:10.1016/j.scriptamat.2022.115056.

References

[1] S.V. Ketov, Y.H. Sun, S. Nachum, Z. Lu, A. Checchi, A.R. Beraldin, H.Y. Bai, W. H. Wang, D.V. Louzguine-Luzgin, M.A. Carpenter, A.L. Greer, Nature 524 (2015) 200–203.
[2] J. Pan, Y.X. Wang, Q. Guo, D. Zhang, A.L. Greer, Y. Li, Nat. Commun. 9 (2018) 560.
[3] X.L. Bian, G. Wang, H.C. Chen, L. Yan, J.G. Wang, Q. Wang, P.F. Hu, J.L. Ren, K. C. Chan, N. Zheng, A. Teresiak, Y.L. Gao, Q.J. Zhai, J. Eckert, J. Beadsworth, K. A. Dahmen, P.K. Liaw, Acta Mater. 106 (2016) 66–77.
[4] J. Saida, R. Yamada, M. Wakeda, Appl. Phys. Lett. 103 (2013), 221910.
[5] K.W. Park, C.M. Lee, M. Wakeda, Y. Shibutani, M.L. Falk, J.C. Lee, Acta Mater. 56 (2008) 5440–5450.
[6] J. Ketkaew, R. Yamada, H. Wang, D. Kuldinow, B.S. Schroers, W. Drnowski, T. Egami, J. Schroers, Acta Mater. 184 (2020) 100–108.
[7] P. Murali, U. Ramamurty, Acta Mater. 53 (2005) 1467–1478.
[8] G. Kumar, D. Rector, R.D. Conner, J. Schroers, Acta Mater. 57 (2009) 3572–3583.
[9] G. Kumar, P. Neibecker, Y.H. Liu, J. Schroers, Nat. Commun. 4 (2013) 1536.
[10] J. Ketkaew, W. Chen, H. Wang, A. Datye, M. Fan, G. Pereira, U.D. Schwarz, Z. Liu, R. Yamada, W. Dmowski, M.D. Shattuck, C.S. O'Hern, T. Egami, E. Bouchbinder, J. Schroers, Nat. Commun. 9 (2018) 3271.
[11] G. Kumar, S. Prades-Rodel, A. Blatter, J. Schroers, Scr. Mater. 65 (2011) 585–587.
[12] S. Di, Q. Wang, J. Zhou, Y. Shen, J. Li, M. Zhu, K. Yin, Q. Zeng, L. Sun, B. Shen, Scr. Mater. 187 (2020) 13–18.
[13] W. Song, X. Meng, Y. Wu, D. Cao, H. Wang, X. Liu, X. Wang, Z. Lu, Sci. Bull. 63 (2018) 840–844.
[14] T.J. Lei, L.R. DaCosta, M. Liu, W.H. Wang, Y.H. Sun, A.L. Greer, M. Atzmon, Acta Mater. 164 (2019) 165–170.
[15] Y. Tang, H. Zhou, H. Lu, X. Wang, Q. Cao, D. Zhang, W. Yang, J.-Z. Jiang, Nat. Commun. 13 (2022) 2120.
[16] W.H. Wang, Prog. Mater. Sci. 106 (2019), 100561.
[17] H.-B. Yu, W.-H. Wang, K. Samwer, Mater. Today 16 (2013) 183–191.
[18] R. Zhao, H.Y. Jiang, P. Luo, L.Q. Shen, P. Wen, Y.H. Sun, H.Y. Bai, W.H. Wang, Phys. Rev. B 101 (2020), 094203.
[19] F. Zhu, A. Hirata, P. Liu, S. Song, Y. Tian, J. Han, T. Fujita, M. Chen, Phys. Rev. Lett. 119 (2017), 215501.
[20] F. Zhu, H.K. Nguyen, S.X. Song, D.P.B. Aji, A. Hirata, H. Wang, K. Nakajima, M. W. Chen, Nat. Commun. 7 (2016) 11516.
[21] Z. Lu, W. Jiao, W.H. Wang, H.Y. Bai, Phys. Rev. Lett. 113 (2014), 045501.
[22] Z. Wang, W.-H. Wang, Natl. Sci. Rev. 6 (2019) 304–323.
[23] K. Geels, D.B. Fowler, W.U. Kopp, M. Rückert, ASTM Int. (2007).
[24] Z. Evenson, R. Busch, J. Alloys Compd. 509 (2011) S38–S41.
[25] I. Gallino, D. Cangialosi, Z. Evenson, L. Schmitt, S. Hechler, M. Stolpe, B. Ruta, Acta Mater. 144 (2018) 400–410.
[26] Z. Evenson, I. Gallino, R. Busch, J. Appl. Phys. 107 (2010), 123529.
[27] H.B. Yu, W.H. Wang, H.Y. Bai, Y. Wu, M.W. Chen, Phys. Rev. B 81 (2010), 220201.

[28] L. Song, W. Xu, J. Huo, J.-Q. Wang, X. Wang, R. Li, Intermetallics 93 (2018) 101–105.
[29] C.T. Moynihan, A.J. Easteal, M.A. Debolt, J. Tucker, J. Am. Ceram. Soc. 59 (1976) 12–16.
[30] A. Datye, J. Ketkaew, J. Schroers, U.D. Schwarz, J. Alloys Compd. 819 (2020), 152979.
[31] Y.Z. Yue, R. von der Ohe, S.L. Jensen, J. Chem. Phys. 120 (2004) 8053–8059.
[32] G.R. Garrett, M.D. Demetriou, M.E. Launey, W.L. Johnson, Proc. Natl. Acad. Sci. U. S. A. 113 (2016) 10257–10262.
[33] P. Saini, R.L. Narayan, J. Alloys Compd. 898 (2022), 162960.
[34] J. Pan, Y.P. Ivanov, W.H. Zhou, Y. Li, A.L. Greer, Nature 578 (2020) 559–562.
[35] F. Zhu, S. Song, K.M. Reddy, A. Hirata, M. Chen, Nat. Commun. 9 (2018).
[36] H. Huang, J. Zhang, C.-H. Shek, J. Yan, J. Alloys Compd. 674 (2016) 223–228.
[37] C. Ebner, S. Pauly, J. Eckert, C. Rentenberger, Mater. Sci. Eng. A 773 (2020), 138848.
[38] A. Bhattacharyya, G. Singh, K.E. Prasad, R. Narasimhan, U. Ramamurty, Mater. Sci. Eng. A 625 (2015) 245–251.
[39] D.P. Wang, J.C. Qiao, C.T. Liu, Mater. Res. Lett. 7 (2019) 305–311.
[40] Y. Wang, P. Li, L.M. Wang, Intermetallics 93 (2018) 197–200.
[41] M.C. Li, M.Q. Jiang, F. Jiang, L. He, J. Sun, Scr. Mater. 138 (2017) 120–123.
[42] Q. Wang, Y. Yang, H. Jiang, C.T. Liu, H.H. Ruan, J. Lu, Sci. Rep. 4 (2014) 4757.
[43] D. Rajpoot, R.L. Narayan, L. Zhang, P. Kumar, H. Zhang, P. Tandaiya, U. Ramamurty, J Mater. Sci. Tchnol. 106 (2022) 225–235.
[44] M.R.J. Gibbs, H.R. Sinning, J. Mater. Sci. 20 (1985) 2517–2525.
[45] Y. Zhu, Y. Zhou, A. Wang, H. Li, H. Fu, H. Zhang, H. Zhang, Z. Zhu, Mater. Sci. Eng. A 850 (2022), 143565.